

# Contribution of Fetal MR Imaging in the Prenatal Diagnosis of Zellweger Syndrome

## CASE REPORT

F. Mochel  
A.-G. Gréville  
A. Benachi  
J. Martinovic  
F. Razavi  
D. Rabier  
I. Simon  
N. Boddaert  
F. Brunelle  
P. Sonigo

**SUMMARY:** Zellweger syndrome (ZS), or cerebrohepato renal syndrome, was the first described peroxisomal biogenesis disorder. It represents the most severe phenotype, and some of its multiple congenital anomalies can manifest prenatally. Fetal hypokinesia, renal hyperechogenicity, and cerebral ventricular enlargement are the most common reported fetal features. Single and/or late detectable manifestations account for most of the difficulties of prenatal diagnosis, as well as the limitations of ultrasonography itself. Prenatal diagnosis, however, can be achieved through (1) assays of concentrations of peroxisomal metabolites (very-long-chain fatty acids, bile acids, intermediates, plasmalogens), (2) activities of peroxisomal enzymes (dihydroacetone-phosphate acyltransferase), or (3) molecular screening techniques, if available. We report on the contribution of MR imaging to the diagnosis of ZS in 2 unrelated fetuses. MR imaging was performed in the third trimester because of cerebral ventricular enlargement diagnosed on routine sonography examinations. In both cases, MR imaging revealed ZS-characteristic abnormal cortical gyral patterns, impaired myelination, and cerebral periventricular pseudocysts. In addition, MR imaging revealed renal microcysts and hepatosplenomegaly in one case. The high level of resolution of MR imaging, which allows analysis of cerebral gyration and myelination, facilitates the prenatal diagnosis of complex polymalformative syndromes such as ZS.

**P**eroxisomal biogenesis involves the synthesis of greater than 50 enzymes that mostly participate in beta-oxidation of fatty acids, synthesis of phospholipids, bile acids, and isoprene compounds.<sup>1,2</sup> As a peroxisomal biogenesis disorder, Zellweger syndrome (ZS) associates elevated plasma, very-long-chain fatty acids (VLCFA),<sup>3</sup> bile acids,<sup>4</sup> phytanic, pristanic,<sup>5</sup> and pipecolic acids contrasting with low plasma plasmalogens.<sup>6</sup> Some impaired enzymatic activity, such as dihydroacetone-phosphate acyltransferase deficiency, can also be detected in fibroblasts of ZS patients.<sup>7</sup> ZS is associated with 11 of the 12 complementation groups comprising the peroxisomal biogenesis disorders.<sup>8,9</sup> Several genes have been identified for each of these groups and constitute the PEX genes family, so molecular analysis can finally confirm the diagnosis of ZS.<sup>10</sup> Because the above analyses can be conducted on cultured chorionic villous cells or cultured amniocytes, a reliable prenatal diagnosis of ZS can be proposed in the presence of a familial history. A few pitfalls in the prenatal diagnosis were reported, but only when a single test was conducted.<sup>11,12</sup>

ZS, also known as the cerebrohepato renal syndrome, is an autosomic recessive disorder that affects about 1/50,000 births.<sup>13</sup> It is the most severe of the peroxisomal biogenesis disorders—death usually occurs within the first year of life—and is characterized by multiple congenital anomalies.<sup>14,15</sup> Its clinical spectrum associates facial dysmorphism with large fontanelle, ophthalmologic defects, neurologic impairment, hepatic disorders, cystic renal malformations, and punctuate calcifications in the patella.<sup>16</sup> Some of these abnormalities—eg, fetal hypokinesia, cerebral ventricular enlargement, or renal hyperechogenicity—can be identified prenatally.<sup>17</sup>

We report on 2 unrelated fetuses for whom the ultrasonographic diagnosis of cerebral ventricular enlargement was ex-

panded by MR imaging findings during the third trimester of pregnancy.

## Case Reports

### Case 1

The female child was born to young, unrelated, white parents. Pregnancy was uneventful, with normal sonographic follow-up at 6, 13, and 24 weeks of amenorrhea. At 35 weeks of amenorrhea, however, sonographic examination showed an isolated and asymmetric ventricular enlargement (right ventricle measured 15 mm at the atrial level). Amniocentesis was then performed with normal standard karyotype and negative virus screening in amniocytes.

The brain MR imaging confirmed the asymmetric ventricular enlargement (the right ventricle measured 16 mm, and the left ventricle measured 11 mm at the atrial level) and showed a large cavum (Fig 1). The MR imaging also revealed important disorders of neuronal migration, with abnormally small cerebral convolutions, mostly in the frontal and in the perisylvian cortex (Fig 1). In addition, abnormality of white matter was observed, with periventricular leukodystrophy predominating in the frontal area as well as germinolytic cysts in the subependymal areas (Fig 1).

The child was born at term, with normal birth parameters but with dysmorphic facial features. Her neurologic examination revealed severe impairment, and sensorineural tests evidenced impaired auditory and visual evoked potentials with altered electroretinogram. Extraneurologic follow-up revealed a symptomatic cardiopathy and renal microcysts but neither hepatosplenomegaly or calcific stippling. The evolution was characterized by rapid neurologic deterioration, with severe epileptic seizures leading to death at 35 days of age.

Biochemical investigations confirmed the diagnosis of ZS with significant elevation of VLCFA and pipecolic acid in plasma, associated with severely reduced dihydroacetone-phosphate acyltransferase activity in fibroblasts.

### Case 2

Young, unrelated, white parents had a previous child who was healthy despite a low birth weight (2400 g). The second pregnancy was uneventful until 22 weeks of amenorrhea, when moderate growth

Received January 7, 2005; accepted after revision April 1.

From the Service de Radiologie Pédiatrique (F.M., I.S., N.B., F.B., P.S.), Service de la Maternité (A.-G.G., A.B.), Service d'Histo-embryologie et de Cytogénétique (J.M., F.R.), and Département de Biochimie (D.R.), Hôpital Necker-Enfants Malades, Paris, France.

Address correspondence to Pascale Sonigo, Service de Radiologie Pédiatrique, Hôpital Necker-Enfants Malades, 149 rue de Sèvres, 75015 Paris, France.

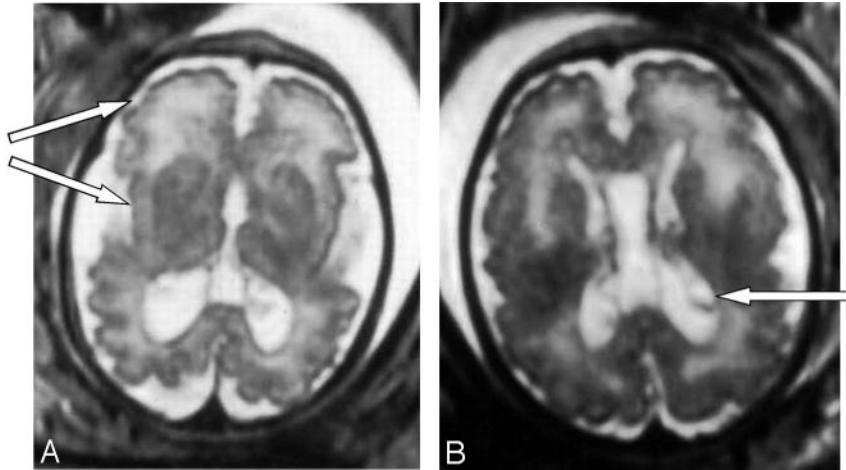


**Fig 1.** Case 1. Axial T2-weighted MR images show bilateral ventriculomegaly as well as large cavum. Abnormally small cerebral convolutions predominate in the frontal and perisylvian cortex (A) and periventricular leukodystrophy predominates in the frontal area. Note bilateral germinolytic cysts in the subependymal areas (B).

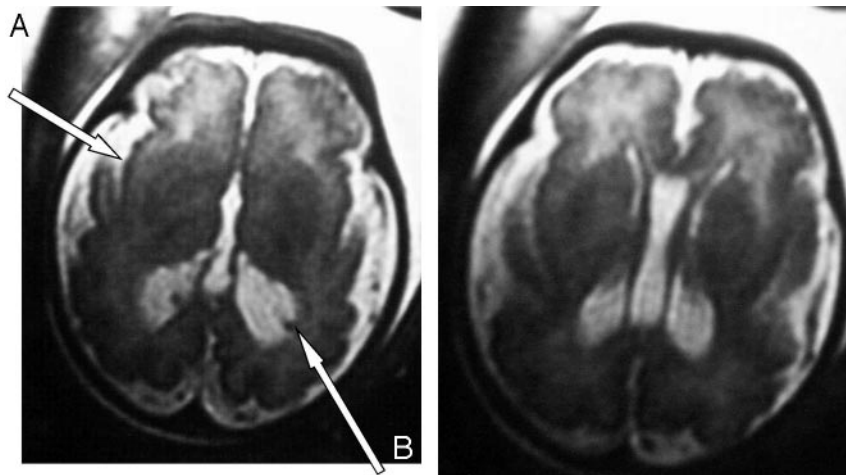


**Fig 2.** Case 2. Axial T2-weighted MR images reveal, as in case 1, bilateral ventricular enlargement, frontal abnormalities of the white matter, and polymicrogyria predominating in the frontal, perisylvian cortex with large sylvian valley (A) and bilateral periventricular pseudocysts (B).

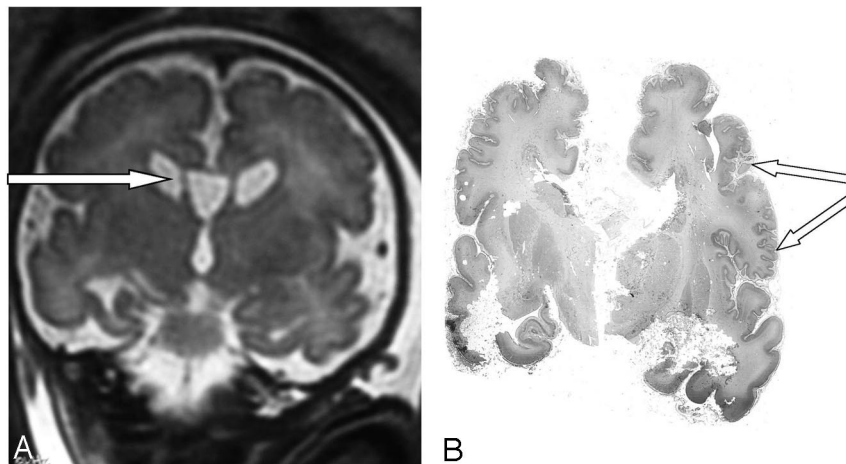


**Fig 3.** Case 2. Coronal T2-weighted MR image shows large cavum and bilateral subependymal pseudocysts (A). Postmortem coronal section confirms the micropolygyric pattern predominating in the frontal and perisylvian cortex (B).

(1) bilateral ventricular enlargement (lateral ventricle measured 16 mm at the atrial level) associated with a large cavum (Figs 2 and 3), (2) abnormal gyration patterns, mostly in the frontal and in the perisylvian cortex (Fig 2), (3) periventricular leukodystrophy, mainly in the frontal area (Fig 2), and (4) irregular ventricular walls revealing bilateral subependymal pseudocysts (Figs 2 and 3).

The parents elected to terminate the pregnancy at 36 weeks. Postmortem examination

retardation was observed (tenth percentile). At 25 weeks of amenorrhea, follow-up sonography revealed a moderate ventricular enlargement (lateral ventricle measured 10 mm at the atrial level). At 30 weeks of amenorrhea, growth retardation was confirmed (between the fifth and the tenth percentile) as well as asymmetric ventricular enlargement (the left ventricle measured 11.5 mm, and the right ventricle 12.5 mm at the atrial level). Amniocentesis was performed with normal standard karyotype and negative virus screening.

At 35 weeks of amenorrhea, a fetal MR imaging showed bilateral renal microcysts, hepatosplenomegaly, and heterogeneous hyposignal of the liver. Brain MR imaging revealed multiple abnormalities:

of the male fetus showed moderate growth retardation with weight at the tenth percentile. The fetus presented dysmorphic features, hepatosplenomegaly, renal cortical microcysts, small adrenals, and multiple calcific stippling of the patellae. Macroscopic examination of the brain revealed moderate ventricular enlargement with large cavum, thin corpus callosum, and small germinolytic cysts. Histopathologic analysis revealed microgyria predominating in the frontal and perisylvian areas (Fig 3). Abnormal gyration patterns were also observed in the inferior olivary nucleus and in the dentate nucleus of the cerebellum, which presented with diffuse heterotopias. ZS was confirmed by a marked elevation of the VLCFA in the amniotic fluid.

## Methods

Fetal MR imaging was performed on a GE signal intensity 1.5T unit.<sup>18</sup> A phased array coil (Torso) was used. Mothers were not premedicated and were placed on the dorsal decubitus, legs slightly folded. A scout image was obtained in a maternal coronal plane with a fast spin-echo (FSE) sequence to localize the fetus.

The study of the cerebral structures was realized on the 3 reference planes in FSE T2 sequences (TE, 120 milliseconds; TR, 8000 milliseconds; ETL, 64; 1 excitation; matrix, 256 × 256; field of view [FOV], from 36 cm to 40 cm; 5-mm section thickness; gap, 2.5 mm) and T1-weighted GE ( $\tau$ , 80°; TE, 5 milliseconds; TR, 250 milliseconds; ETL, 12; 1 excitation; matrix, 256 × 256; FOV, 36 cm to 40 cm; 5-mm section thickness; gap, 2.5 mm; acquisition time, 40 seconds). In case of movement artifacts, T2-weighted single-shot sequences were used (TE, 90 milliseconds; TR, 2165 milliseconds; BW, 31.25; matrix, 384 × 192; 5-mm section thickness; gap, 0).

Brain examination included the size of the ventricles, the features of the ventricular walls (subependymal cysts), the white matter signal intensity, and the gyration pattern. At the thoracoabdominal level, the sequences were performed in the axial and coronal T2 planes, as well as in the sagittal and coronal T1 planes, to analyze the kidneys, the liver, the spleen, and the hypersignal originating from colic meconium (“barium enema” aspect).

## Discussion

Because ZS is characterized by multiple congenital anomalies (renal, hepatic, and skeletal), the most discriminant features lie in the cerebral abnormalities. Indeed, histopathologic analyses of the brain are consistent with 3 typical features: neuronal migration abnormalities, white matter abnormalities, and selective neuronal involvement.<sup>19-21</sup>

Abnormalities in neuronal migration of ZS are characterized by a unique combination of centrosylvian pachygyria-polymicrogyria.<sup>22</sup> Pachygyria affects medial gyri around the perirolandic area, whereas polymicrogyria occurs more laterally, close to the frontal and the perisylvian cortex.<sup>23</sup> Another unique feature of the Zellweger malformation is the laminar discontinuity in the principal olivary nucleus, which might result from a discontinuity in the laminar organization of the Purkinje cells. This discontinuity is responsible for the classic cerebellar heterotopias described in this syndrome.<sup>21</sup> Whereas cytoarchitectural analyses revealed irregular neuronal arrangement with delayed maturation, poor dendritic arborization, and poor spine development,<sup>24</sup> it is not clear why only a fraction of the neurons of a given class fails to complete migration. Recently, Infante and Huszagh suggested that the decrease in docosahexaenoic acid—and the secondary carnitine deficiency—reported in ZS could be responsible for the impairment in the neuronal migration.<sup>25</sup> The partial disturbance of migration of multiple neuronal classes observed, however, may imply that migration is disturbed at an early stage of cortical histogenesis—ie, between the third and sixth months of pregnancy.<sup>21</sup> This would be consistent with the dysplastic cerebral alterations observed on a fetus interrupted at 21 weeks of gestation in the context of a familial history of ZS.<sup>26</sup>

In addition, in light of the early occurrence of abnormalities of the white matter, the term “dysmyelination” is probably more appropriate to characterize the maturational disorder in myelination,<sup>27</sup> which affects the periventricular region from the posterior sylvian to the frontoparietal area.<sup>23</sup> Conversely,

in neonatal adrenoleukodystrophy—a similar disorder of peroxisomal biogenesis—demyelination occurs associated with an inflammation reaction. This makes possible a differential diagnosis with ZS.<sup>27</sup> The physiopathology of this severe myelin deficiency, however, is still debated. The accumulation of sudanophilic lipids has led to the conclusion of a sudanophilic leukodystrophy,<sup>19</sup> whereas lamellar inclusions in both the white and gray matter were found to contain cholesterol esterified associated with VLCFA. Consequently, the white matter abnormalities in ZS may be related to the defect in VLCFA metabolism, as it was also hypothesized in X-linked ALD.<sup>28</sup> Others suggested a disorder of migration itself,<sup>22</sup> or the decrease in main components of the myelin such as plasmalogens<sup>23</sup> or docosahexaenoic acid.<sup>25</sup>

These different neuropathologic findings are consistent with the imaging patterns observed in brain MR imaging of ZS patients. After the first description made by van der Knaap and Valk<sup>27</sup> and Barkovich et al<sup>23</sup> and others<sup>29,30</sup> confirmed the combination of characteristic findings—namely, cortical malformations of the perisylvian and perirolandic regions, hypomyelination, and germinolytic cysts. The only report of a patient suspected of ZS without cortical and myelination abnormalities was ruled out after careful interpretation of the MR imaging pattern.<sup>31</sup> Therefore, in light of the severity and the precocity of the various malformations in ZS,<sup>26</sup> it is not surprising to observe manifestations that can be detected prenatally by standard ultrasound investigations. However, in view of its high level of resolution, fetal MR imaging is the only technique able to detect the specific combination of migration and myelination abnormalities, and should be performed in between the twenty-eighth and the thirty-fourth weeks of amenorrhea—unlike our cases—for better analysis.<sup>18</sup> Indeed, before 28 weeks of amenorrhea, the superiority of brain MR imaging over ultrasound examination has not been proved, whereas after 34 weeks of amenorrhea the reduction of the subarachnoid space does not allow a good delineation of the sulci.<sup>32</sup> However, because of the association of microgyria with periventricular leukodystrophy and germinolytic cysts, a viral infection was first suspected in case 1, even if cerebral lesions are usually of less specific localization. Indeed, congenital cytomegalovirus infection is the most frequent affection known to manifest prenatally with both polymicrogyria and dysmyelination.<sup>33</sup> Apart from peroxisomal biogenesis disorders, few inborn errors of metabolism—principally respiratory chain defect<sup>34</sup> and pyruvate dehydrogenase deficiency<sup>35</sup>—have been described prenatally with both gyration and myelination abnormalities. Moreover, other genetic disorders presenting postnatally with polymicrogyria and dysmyelination—such as Walker Warburg syndrome<sup>36</sup> or Fukuyama syndrome<sup>37</sup>—have not been reported yet with prenatal radiologic findings. Therefore, after eliminating a viral infection, the recurrence of such a specific MR imaging pattern, together with hepatorenal features, led to the high suspicion of ZS in case 2. The diagnosis was confirmed by fetopathologic examination and biochemical investigations.

In conclusion, ZS is a severe polymalformative pattern that leads to death in the first months of life as few therapeutic perspectives are actually available. Our 2 cases emphasize the possibility of prenatal manifestations of ZS that can be diagnosed on fetal MR imaging. The association of cerebral anom-

alies such as micro- or pachygyria, periventricular leukodystrophy and germinolytic cysts are highly suggestive of a disorder of peroxisomal biogenesis. The presumption of ZS is even stronger when localized to the centrosylvian region or when associated to renal and/or hepatic abnormalities. Therefore, when nonspecific defects are detected on routine sonography examination, prenatal MR imaging can contribute to the positive diagnosis of peroxisomal biogenesis disorders. The diagnosis is then confirmed by biochemical and/or molecular investigations. These reliable prenatal laboratory tests can be proposed to parents; however, the late recognition of such anomalies in the third trimester can be an important restriction to the prenatal investigations of the ongoing pregnancy.

## References

- van den Bosch H, Schutgens RB, Wanders RJ, et al. Biochemistry of peroxisomes. *Annu Rev Biochem* 1992;61:157–97
- Wanders RJ, Tager JM. Lipid metabolism in peroxisomes in relation to human disease. *Mol Aspects Med* 1998;19:69–154
- Moser AE, Singh I, Brown FR 3rd, et al. The cerebrohepatorenal (Zellweger) syndrome: increased levels and impaired degradation of very-long-chain fatty acids and their use in prenatal diagnosis. *N Engl J Med* 1984;310:1141–46
- Setchell KD, Vestal CH. Thermospray ionization liquid chromatography-mass spectrometry: a new and highly specific technique for the analysis of bile acids. *J Lipid Res* 1989;30:1459–69
- ten Brink HJ, Wanders RJ, Stellaard F, et al. Pristanic acid and phytanic acid in plasma from patients with a single peroxisomal enzyme deficiency. *J Inherit Metab Dis* 1991;14:345–48
- Wanders RJ, Purvis YR, Heymans HS, et al. Age-related differences in plasmalogen content of erythrocytes from patients with the cerebro-hepato-renal (Zellweger) syndrome: implications for postnatal detection of the disease. *J Inherit Metab Dis* 1986;9:335–42
- Wanders RJ, Ofman R, Romeijn GJ, et al. Measurement of dihydroxyacetone-phosphate acyltransferase (DHAPAT) in chorionic villous samples, blood cells and cultured cells. *J Inherit Metab Dis* 1995; 18 (suppl 1):90–100
- Brul S, Westerveld A, Strijland A, et al. Genetic heterogeneity in the cerebro-hepatorenal (Zellweger) syndrome and other inherited disorders with a generalized impairment of peroxisomal functions: a study using complementation analysis. *J Clin Invest* 1988;81:1710–15
- Shimozawa N, Suzuki Y, Orii T, et al. Standardization of complementation grouping of peroxisome-deficient disorders and the second Zellweger patient with peroxisomal assembly factor-1 (PAF-1) defect. *Am J Hum Genet* 1993;52: 843–44
- Gould SJ, Valle D. Peroxisome biogenesis disorders: genetics and cell biology. *Trends Genet* 2000;16:340–45
- Carey WF, Poulos A, Sharp P, et al. Pitfalls in the prenatal diagnosis of peroxisomal beta-oxidation defects by chorionic villus sampling. *Prenat Diagn* 1994;14:813–19
- Moser AB, Rasmussen M, Naidu S, et al. Phenotype of patients with peroxisomal disorders subdivided into sixteen complementation groups. *J Pediatr* 1995;127:13–22
- Danks DM, Tippett P, Adams C, et al. Cerebro-hepato-renal syndrome of Zellweger: a report of eight cases with comments upon the incidence, the liver lesion, and a fault in pipecolic acid metabolism. *J Pediatr* 1975;86:382–87
- Kelley RI. Review: the cerebrohepatorenal syndrome of Zellweger, morphologic and metabolic aspects. *Am J Med Genet* 1983;16:503–17
- Wilson GN, Holmes RG, Custer J, et al. Zellweger syndrome: diagnostic assays, syndrome delineation, and potential therapy. *Am J Med Genet* 1986;24:69–82
- Gould SJ, Raymond GV, Valle D. Lactic acidemia. In: Scriver CR, Beaudet AL, Sly WS, et al, eds. *The metabolic basis of inherited diseases*. Vol 2. 8th ed. New York: McGraw-Hill;2001:2275–95
- Johnson JM, Babul-Hirji R, Chitayat D. First-trimester increased nuchal translucency and fetal hypokinesia associated with Zellweger syndrome. *Ultrasound Obstet Gynecol* 2001;17:344–46
- Sonigo PC, Rypens FF, Carteret M, et al. MR imaging of fetal cerebral anomalies. *Pediatr Radiol* 1998;28:212–22
- Passarge E, McAdams AJ. Cerebro-hepato-renal syndrome: a newly recognized hereditary disorder of multiple congenital defects, including sudanophilic leukodystrophy, cirrhosis of the liver, and polycystic kidneys. *J Pediatr* 1967;71:691–702
- Volpe JJ, Adams RD. Cerebro-hepato-renal syndrome of Zellweger: an inherited disorder of neuronal migration. *Acta Neuropathol (Berl)* 1972;20:175–98
- Evrard P, Caviness VS Jr, Prats-Vinas J, et al. The mechanism of arrest of neuronal migration in the Zellweger malformation: an hypothesis based upon cytoarchitectonic analysis. *Acta Neuropathol (Berl)* 1978;41:109–17
- Powers JM, Moser HW. Peroxisomal disorders: genotype, phenotype, major neuropathologic lesions, and pathogenesis. *Brain Pathol* 1998;8:101–20
- Barkovich AJ, Peck WW. MR of Zellweger syndrome. *AJNR Am J Neuroradiol* 1997;18:1163–70
- Takashima S, Chan F, Becker LE, et al. Cortical cytoarchitectural and immunohistochemical studies on Zellweger syndrome. *Brain Dev* 1991;13:158–62
- Infante JP, Huszagh VA. On the molecular etiology of decreased arachidonic (20:4n-6), docosapentaenoic (22:5n-6) and docosahexaenoic (22:6n-3) acids in Zellweger syndrome and other peroxisomal disorders. *Mol Cell Biochem* 1997;168:101–15
- Powers JM, Moser HW, Moser AB, et al. Fetal cerebrohepatorenal (Zellweger) syndrome: dysmorphic, radiologic, biochemical, and pathologic findings in four affected fetuses. *Hum Pathol* 1985;16:610–20
- van der Knaap MS, Valk J. The MR spectrum of peroxisomal disorders. *Neuroradiology* 1991;33:30–37
- Powers JM, Tummons RC, Moser AB, et al. Neuronal lipidosis and neuroaxonal dystrophy in cerebro-hepato-renal (Zellweger) syndrome. *Acta Neuropathol (Berl)* 1987;73:333–43
- Nakai A, Shigematsu Y, Nishida K, et al. MRI findings of Zellweger syndrome. *Pediatr Neurol* 1995;13:346–48
- Panjan DP, Meglic NP, Neubauer D. A case of Zellweger syndrome with extensive MRI abnormalities and unusual EEG findings. *Clin Electroencephalogr* 2001;32:28–31
- Stone JA, Castillo M. MR in a patient with Zellweger syndrome presenting without cortical or myelination abnormalities. *AJNR Am J Neuroradiol* 1998; 19:1378–79
- Garel C, Chantrel E, Elmaleh M, et al. Fetal MRI: normal gestational landmarks for cerebral biometry, gyration and myelination. *Childs Nerv Syst* 2003;19: 422–25
- Barkovich AJ, Lindan CE. Congenital cytomegalovirus infection of the brain: imaging analysis and embryologic considerations. *AJNR Am J Neuroradiol* 1994;15:703–15
- Samson JF, Barth PG, de Vries JJ, et al. Familial mitochondrial encephalopathy with fetal ultrasonographic ventriculomegaly and intracerebral calcifications. *Eur J Pediatr* 1994;153:510–16
- Moroni I, Bugiani M, Bizzi A, et al. Cerebral white matter involvement in children with mitochondrial encephalopathies. *Neuropediatrics* 2002;33: 79–85
- van der Knaap MS, Smit LM, Barth PG, et al. Magnetic resonance imaging in classification of congenital muscular dystrophies with brain abnormalities. *Ann Neurol* 1997;42:50–59
- Kato T, Funahashi M, Matsui A, et al. MRI of disseminated developmental dysmyelination in Fukuyama type of CMD. *Pediatr Neurol* 2000;23:385–88